



14TH CANADIAN MASONRY SYMPOSIUM
MONTREAL, CANADA
MAY 16TH – MAY 20TH, 2021



**ANCHOR BOLT PERFORMANCE IN CMU ASSEMBLIES WITH LIGHTWEIGHT
GROUT**

Shrestha, Rumi¹; Kessler, Hannah²; Redmond, Laura³ and Rangaraju, Prasad⁴

ABSTRACT

Reduction in structural mass, improvement in thermal performance, and reduction in shrinkage cracking through internal curing are some of the reasons that lightweight aggregates have been used in structures and pavements for decades. However, lightweight grout is still not permitted for use in reinforced masonry construction by the TMS 402-16 code. In order to realize the benefits of lightweight grout in U.S. reinforced masonry construction, a codified procedure for its use is required which must be informed by experimental testing. The objective of this paper is to study the behavior of anchor bolts under tension within CMU assemblies constructed with two types of lightweight grout, one with expanded clay aggregates and the other with expanded slate aggregates and determine if current TMS 402-16 equations are appropriate to predict design capacity. Ten CMU wall panels (5 specimens for each lightweight grout type), fully grouted with lightweight grout and cast-in-place bent bar anchors, were constructed and tested in static out-of-plane tension in accordance with ASTM E488 as permitted in TMS 402-16. The TMS 402-16 predicted capacities are found to be conservative compared to the tested capacities of the specimens. Additional discussion is provided to compare the results of this dataset to previous studies of lightweight concrete and lightweight grout in the literature and suggest next steps towards codifying the use of lightweight masonry grout.

KEYWORDS: *anchor bolt test, bent bar anchors, lightweight aggregates, lightweight grout*

¹ Graduate Research Assistant, Glenn Department of Civil Engineering, Clemson University, S Palmetto Blvd., Clemson, SC, USA, rshrest@clemson.edu

² Graduate Research Assistant, Glenn Department of Civil Engineering, Clemson University, S Palmetto Blvd., Clemson, SC, USA, hfdilli@clemson.edu

³ TMS Member, Assistant Professor, Glenn Department of Civil Engineering, Clemson University, S Palmetto Blvd., Clemson, SC, USA, lmredmo@clemson.edu

⁴ Professor, Glenn Department of Civil Engineering, Clemson University, S Palmetto Blvd., Clemson, SC, USA, prangar@clemson.edu

INTRODUCTION

Lightweight aggregates can be defined as aggregates with a particle density less than 2000 kg/m³ or a dry loose bulk density less than 1200 kg/m³ [1]. Recently, lightweight aggregates have been used in lightweight concrete production to reduce structural weight, improve thermal insulation, and increase fire resistance [2-5]. Also, in recent years presaturated light-weight aggregate has been used as an internal curing agent to minimize autogenous shrinkage in grouts, mortars and concrete that are typically characterized by low water-to-cementitious (w/cm) materials ratio [6-9]. Lightweight grouts are not as ubiquitous as normal weight grouts in masonry construction, mostly because of the lack of codified procedure for its use. Lightweight aggregates in concrete production have been shown to affect the tensile strength, shear strength, friction properties, splitting resistance, bond between concrete and reinforcement, and development length compared with normal weight concrete of the same compressive strength. Similar testing of these properties in masonry specimens constructed with lightweight grout is needed before a codified procedure can be established. Petty and Nelson [10] designed lightweight grouts using blast furnace steel slag aggregate whose axial tensile strength, compressive strength, and shrinkage performances were comparable to, or if not better than normal-weight grouts. Tanner [11] maintained that tests on grout containing expanded shale aggregate that included determination of slump, unit weight, air content and segregation, when compared to masonry code and ASTM standards, were in an acceptable range. Polanco [12] also performed experiments on expanded shale grout and found it to comply with the requirements of ASTM C476 for making lightweight grout. Tests to determine hardened grout properties including modulus of rupture, axial tensile strengths, etc. were conducted on crushed lightweight sand and natural sand as fines and pea gravel, limestone, and expanded slate lightweight aggregate as coarse by Bane [13]. Though Petty and Nelson have previously conducted some testing of the axial tensile strength of bent-bar anchors, it was based on a modified test method [14] which used wall prisms instead of wall panels for the test and only considered one grout type. Bane also conducted axial tensile strength testing following the test methods of Petty and Nelson, but only three test results were reported because of imprecise strain gage readings caused by eccentric loading of the load cell [13]. Thus, the objective of this study is to conduct anchor bolt pull-out tests using a device designed to mimic the ASTM E488 apparatus for two types of lightweight grouts, one composed of only expanded clay aggregates and one composed of only expanded slate aggregates, that will aid in developing a codified procedure for the use of lightweight grout in masonry construction.

Anchor bolts can be primarily classified into cast-in-place anchors and post-installed anchors. Bent bar cast-in-place anchors are one of the most commonly used and are usually available in “L” and “J” shapes. Allowable stress design or strength design of anchor bolts can be followed to design the anchor bolts. The following nominal tensile strength equations [15] have been found to give the best prediction of bent-bar anchor strength [16]:

$$B_{anb} = 0.332A_{pt}\sqrt{f'_m} \text{ (N, mm)}; B_{anb} = 4A_{pt}\sqrt{f'_m} \text{ (lbf, in.)} \quad (\text{TMS 402-16 Equation 9-3})$$

$$B_{anp} = 1.5f'_m e_b d_b + 2.07\pi(l_b + e_b + d_b)d_b \text{ (N, mm)};$$

$$B_{anp} = 1.5f'_m e_b d_b + 300\pi(l_b + e_b + d_b)d_b \text{ (lbf, in.)} \quad (\text{TMS 402-16 Equation 9-4})$$

$$B_{ans} = A_b f_y \text{ (N, mm or lbf, in.)} \quad (\text{TMS 402-16 Equation 9-5})$$

Where, B_{anb} (N (lbf)) is the tensile strength of a bent-bar anchor bolt governed by tensile cone breakout of the masonry. B_{anp} (N (lbf)) is the tensile strength of a bent-bar anchor bolt governed by straightening and pull out of the bent-bar anchor. B_{ans} (N (lbf)) is the tensile strength of a bent-bar anchor bolt governed by yield of the anchor steel. A_{pt} (mm^2 (in.^2)) is the projected tension area on masonry surface of a right circular cone. f'_m (MPa (psi)) is specified compressive strength of clay masonry or concrete masonry. e_b (mm (in.)) is the projected leg extension of bent-bar anchor. d_b (mm (in.)) is the nominal diameter of reinforcement or anchor bolt. l_b (mm (in.)) is the effective embedment length of headed or bent anchor bolts. A_b (mm^2 (in.^2)) is the cross-sectional area of an anchor bolt and f_y (MPa (psi)) is the specified yield strength of steel for reinforcement and anchors.

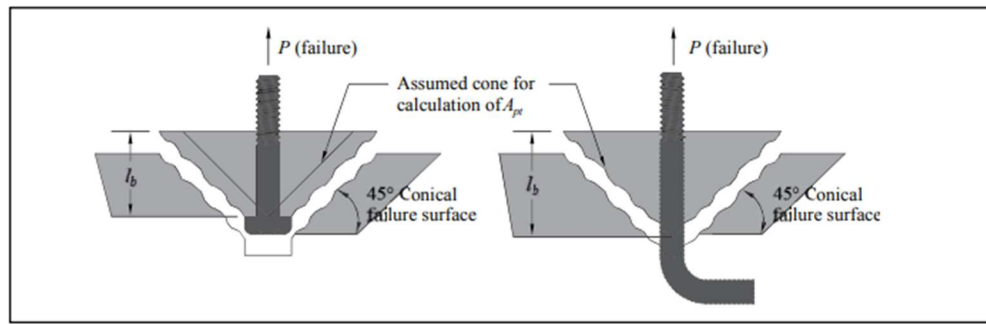


Figure 1: Anchor bolt tensile break out cone [TMS 402/602-16]

In this study, the primary focus was to determine the extent to which the breakout capacity of grouted assemblies constructed with lightweight grout containing cast-in-place bent-bar anchors aligned with the capacities predicted by the strength design equation 9-3 in TMS 402-16. For these tests, the specimens were explicitly designed to force masonry tensile breakout failure (fig. 1).

The organization of the paper is as follows: the experimental program section includes the materials analysis, specimen design and construction, and test set up; the results and discussion section compares the results to previous studies of lightweight concrete and lightweight grout in the literature; the conclusion section provides the major conclusions of the study and the next steps towards codifying the use of lightweight masonry grout.

EXPERIMENTAL PROGRAM

Materials

Two types of lightweight grout mixtures with two different types of lightweight aggregates – expanded clay lightweight aggregates from Arcosa and expanded slate lightweight aggregates from Stalite – were created for this study. Holcim Portland Cement I/II was used as a binding agent for both mixtures. Type S masonry cement mortar was used to assemble the specimens. The

concrete masonry units (CMU) consisted of 20 cm (8 in.) block which were tested (as per ASTM C140) and the unit strength was reported to be 18.3 MPa (2650 psi) as shown in table 1.

Table 1: Unit strength test results

	Net Compressive Strength, MPa (psi)	Gross Compressive Strength, MPa (psi)
Unit 1	17.9 (2600)	9.6 (1390)
Unit 2	18.4 (2670)	10.4 (1510)
Unit 3	15.8 (2290)	8.9 (1290)
Unit 4	20.9 (3030)	11.7 (1700)
Average	18.3 (2650)	10.2 (1470)
Std. Dev.	2.1 (300)	1.2 (180)
Coe. of Var.	11%	12%

Sieve analysis was done per ASTM C136 and the gradation of all aggregates complied with ASTM C330 grading requirements. Specific gravity and absorption tests were also conducted in accordance with ASTM C127 and ASTM C128 for coarse and fine aggregates respectively.

Table 2: Physical Properties of aggregates

Physical property	Expanded clay coarse	Expanded clay fines	Expanded slate coarse	Expanded slate fines
Relative density (OD)	0.92	0.88	1.44	1.75
Relative density (SSD)	1.17	1.35	1.55	2
Specific Gravity (SG)	1.17	1.35	1.55	2
Absorption (%)	27.49	52.68	7.87	14.5
Gradation				
Sieve size	Cumulative % weight by passing			
1/2 in	100	100	100	100
3/8 in	100	100	97.4	100
#4	30.6	100	9.3	100
#8	2.1	69.8	6.9	93.4
#16	1.3	43.6	5.8	41.9
#50	0.8	13.9	5.3	23.8
#100	0.5	9.8	4.9	10.4
#200	0.2	-	2.8	-

Mix proportions and procedure

Mix proportions for both the mixes were in compliance with C476. The proportions were established through a number of trial batches to target at least a 21 MPa (3000 psi) compressive strength at 28-days, which exceeded the required minimum compressive strength of 2000 psi and have a mix that met the required slump of 20 to 28 cm (8 to 11 in.) as specified in ASTM C476.

In the mix design, the aggregates were considered to be in saturated surface dry (SSD) condition. Both the coarse and fine aggregates were soaked in water for 72 hours and were drained by laying them over screens for 24 hours. Prewetting the aggregates to saturated conditions is desirable to ensure internal curing that helps in shrinkage cracking reduction and strengthening of the aggregate-cement bond, which in turn helps increase the grout strength [12]. Coarse aggregates were brought to SSD condition by using paper towels to remove excess moisture on the surface until the paper towel absorbed little to no water. Because the fines were very difficult to bring to precisely SSD condition, the free water content was calculated from a sample of the saturated fine aggregates on each day of mixing and the additional free water in the aggregates was deducted from the total water to be added per the mix design that assumed SSD condition of all the aggregates. The mix proportions were based on ACI mix design procedure [17] and considered the specific gravity of the cement to be 3.15. Calculating the volume proportions of the cement based on bulk unit weight of cement in accordance with definitions in ASTM C476, the resulting mix proportions by volume for both mixes are 1:1.08:0.48 (cement: fines: coarse). Water was added to achieve between a 20 cm (8 in.) and 23 cm (9 in.) slump. The resulting mix design is compliant with the specified strength requirements of ASTM C476 4.2.1.2.

Test specimens

Twelve wall panels (six for each type of aggregate and one spare each) were constructed with the help of a mason for anchor bolt axial tension tests. The test panels were 60 cm X 60 cm (24 in. X 24 in.) wall panels constructed with 20 cm (8 in.) CMU blocks. The wall panels were grouted in 6 different batches due to limits on mixer capacity, and separate ASTM C1019 compression specimens were cast with each batch. Prior to grouting, around 15/16” holes were drilled and the 2 cm (3/4 in.) through the face shells of the blocks, bent bars (L bolts) were embedded to 8 cm (3.125 in.) of effective embedment depth. This combination of embedment length and bar diameter ensured the nominal tension capacity to be given by the masonry tensile breakout equation (TMS 402-16 equation 9-3) was significantly lower than the predicted strengths for anchor bolt straightening/pull out or yielding of the anchor.



Figure 2: a) Anchor bolt test wall panels b) Formwork for compression test specimen

The block arrangement used to cast the ASTM C1019 prisms is shown in figure 2(b) and this permitted realistic absorption of water by the CMU blocks. Two wall panels were grouted per

batch and are designated by batch name-specimen number (i.e. AABT1-1, AABT1-2). The results of slump tests for every batch fell between the desired 20 to 23 cm (8 to 9 in.) per the mix design.

Test procedure

The testing apparatus was designed to mimic the ASTM E488 apparatus for concrete anchor bolt testing. The panels (1 in figure 3(b)) to be tested were laid down on the test floor and any high points from the mortar joints were removed with a file to form a level surface. The panel was prevented from shifting laterally by bracket supports attached to the strong floor of the laboratory. Next, neoprene strips (2 in figure 3(b)) were placed on top of the masonry specimen to form a rectangular window 28 cm X 28 cm (11 in. x11 in.) over which a 15cm (6 in.) thick wooden frame (3 in figure 3(b)) was placed. Great care was taken to level and shim up the surface between the wooden frame and the masonry panel so that the wall would be evenly supported on all sides. The purpose of the wooden frame support was to prevent global flexural failure of the panel while being supported well outside the expected break out cone. Next, the steel loading plate (4 in figure 3(b)) was placed over the anchor bolt and tightened down with a nut. The large loading frame (5 in figure 3(b)) was then placed on top of the wooden frame and the loading rod (6 in figure 3(b)) was attached to the steel loading plate and threaded through the loading frame and large (326 kN capacity) hollow-core hydraulic actuator (7 in figure 3(b)). The top plate (8 in figure 3(b)) was then secured down with a nut to minimize slip during testing. For each test, the loading rate was adjusted such that the specimen failed within 1 to 3 minutes of load application. Four linear potentiometers were used to record the displacement; two of them recorded the displacement of the anchor relative to the wooden frame, and two of them recorded the deflection of the wooden frame relative to the masonry specimen. A digital pressure gauge was calibrated to determine the force in the hydraulic actuator and the signals from the pressure gauge and linear potentiometers were recorded using an NI DAQ.

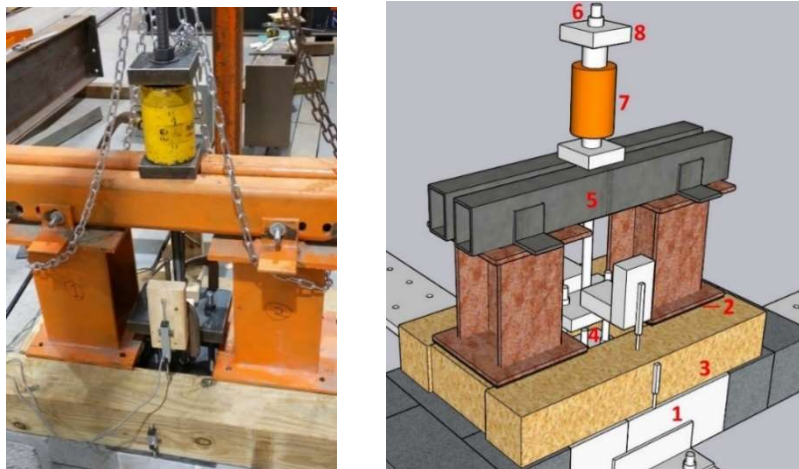


Figure 3: a) Anchor bolt pull-out test setup b) Anchor bolt pull-out test setup (SketchUp)

RESULTS AND DISCUSSION

Grout strength test results

Following table 3 shows the grout strength test results:

Table 3: Grout strength test results

Type	Specimen name	As built compressive strength, MPa (psi) (f_g)
Expanded clay	AABT1-1	24.4 (3540)
	AABT1-2	19.8 (2870)
	AABT3-1	23.3 (3380)
	AABT3-2	25.5 (3700)
	AABT5-1	24.7 (3580)
Expanded slate	SABT1-1	40.9 (5930)
	SABT1-2	30.3 (4390)
	SABT3-1	26.0 (3770)
	SABT5-1	35.6 (5160)
	SABT5-2	31.4 (4550)

Anchor bolt test results

As expected, all specimens experienced primarily masonry tensile breakout failure. Upon inspection of each specimen, the radial cracks emanated from the bolt, but the bolt itself was undamaged, then cracks continued to propagate outwards and split the masonry along the mortar joints. For few specimens, the load was applied for some time even after peak load was achieved to observe the whole core breakout as shown in figures 4(b) and 5(b). The test results revealed that primarily masonry breakout had occurred rather than a flexural failure of the global assembly, anchor yielding, or anchor pull out, as desired per the design of the test.



Figure 4: a) Radial cracks AABT5-1 b) Break out cone and splitting along the mortar



Figure 5: a) Radial cracks in SABT3-1 b) Break out cone with the anchor bolt undisturbed

Using the unit strength method [15] for determining f'_m , the predicted nominal anchor bolt strengths due to masonry tensile break out (TMS 402-16 eq. 9-3), steel yielding (TMS 402-16 eq. 9-5), and straightening and pull out of the bent-bar anchor (TMS 402-16 eq. 9-4) are compared to the tested values of axial tensile strength for each specimen in table 4.

Table 4: Actual axial tensile strengths and predicted axial tensile strengths based on unit strength method (taking $f'_m=10.1$ MPa (2269 psi))

Type	Specimens	Tested tensile strength, kN (lb)	Predicted anchor yield strength, kN (lb)	Predicted anchor pull out strength, kN (lb)	Predicted masonry break out strength, kN (lb)	Tested axial tensile strength / predicted masonry breakout strength
Expanded clay	AABT1-1	29.9	70.7	55.6	26.0	1.15
		(6725)	(15896)	(12515)	(5843)	
	AABT1-2	31.5	70.7	55.6	26.0	1.21
		(7086)	(15896)	(12515)	(5843)	
	AABT3-1	29.1	70.7	55.6	26.0	1.12
		(6558)	(15896)	(12515.1)	(5843)	
AABT3-2	29.6	70.7	55.6	26.0	1.14	
	(6650)	(15896)	(12515)	(5843)		
AABT5-1	31.7	70.7	55.6	26.0	1.22	
	(7123)	(15896)	(12515)	(5843)		
Expanded slate	SABT1-1	53.0	70.7	55.6	26.0	2.04
		(11925)	(15896)	(12515)	(5843)	
	SABT1-2	55.6	70.7	55.6	26.0	2.14
		(12488)	(15896)	(12515)	(5843)	
	SABT3-1	44.0	70.7	55.6	26.0	1.69
		(9902)	(15896)	(12515)	(5843)	
	SABT5-1	53.7	70.7	55.6	26.0	2.07
		(12081)	(15896)	(12515)	(5843)	
	SABT5-2	47.8	70.7	55.6	26.0	1.84
		(10743)	(15896)	(12515)	(5843)	

The TMS 402-16 equations correctly predicted the observed masonry break out failure but all specimens exhibited greater strength than would be predicted by the TMS 402-16 equation for masonry breakout strength. This is somewhat expected, as the masonry tensile breakout equations are conservatively formulated with respect to f'_m even though the failure may often be dominated by the grout.

The proximity of the tested axial tensile strengths of the bent-bar anchors to the predicted axial tensile strengths using the compressive strengths of the grout tested as per ASTM C1019, f'_g , in place of f'_m in the TMS 402-16 equation 9-3 substantiated the assertion of grout dominated failure in the wall panels. The tested axial tensile strengths of the expanded clay specimens were 3% to 11% less than the modified predicted strengths using f'_g , in place of f'_m in the TMS 402-16 equation 9-3. The tested axial tensile strengths of the expanded slate specimens were 26% to 54% greater than the modified predicted strengths using f'_g , in place of f'_m in the TMS 402-16 equation 9-3. The higher axial tensile strengths of the anchors cast in the expanded slate specimens compared to the anchors cast in the expanded clay specimens is partly attributable to the higher compressive strength of the former to the latter. However, the difference between the actual axial tensile strengths and predicted axial tensile strengths for the expanded clay specimens were found to be much lower than that for the expanded slate specimens suggests more than just the difference in compressive strengths between the two types of specimens caused the significant increase in masonry breakout capacity for the expanded slate specimens.

To ensure that the relative tensile to compressive strength of the expanded slate grout were higher compared to the expanded clay grout, additional modulus of rupture testing (ASTM E518) with small beams were conducted using the same grout mix designs as used in the anchor bolt testing. Literature data from lightweight concrete [18], lightweight grout [13], and our test data of the expanded clay and expanded slate grouts are collated to plot the graphs in fig. 6(a) and fig. 6(b). For the modulus of rupture (f_r) vs. compressive strength (f'_c or f'_g) graph as shown in fig. 6(a), a trend line for the lightweight concrete data has been drawn to visualize how far the modulus of rupture values for grout are from the trend line.

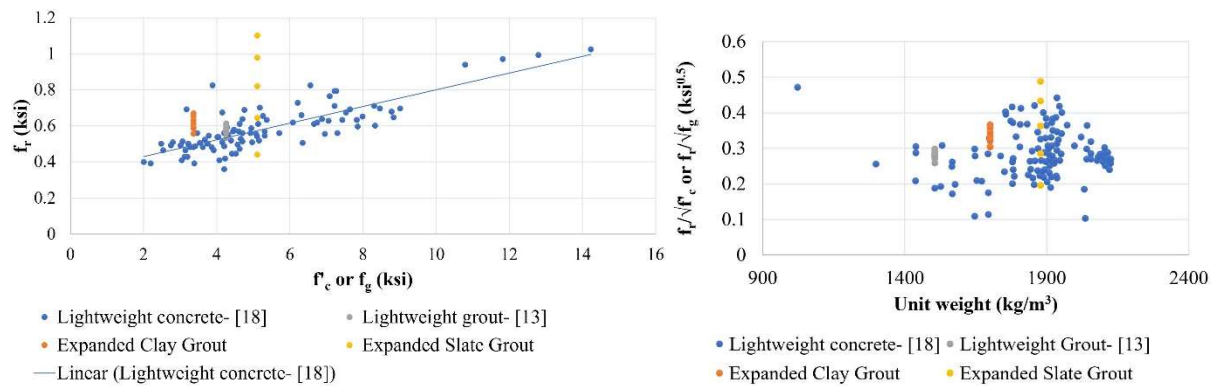


Figure 6: (a) f_r vs f'_c or f'_g graph (b) $f_r/\sqrt{f'_c}$ or $f_r/\sqrt{f'_g}$ vs unit weight graph

The modulus of rupture values for the expanded clay specimens seem much closer to the trend line in comparison to that for the expanded slate specimens. This corroborates the higher deviation and spread of actual axial tensile strengths of the expanded slate specimens with respect to their predictive axial tensile strength. In addition, the mean of the f_r value vs. compressive strength of the expanded slate specimens is higher than the expanded clay specimens, which is in agreement with the larger difference between the actual and predicted axial tensile strengths for the expanded slate specimens. Test data suggest correlation between the aggregate type and the relative strength of the mix in tension with the expanded slate exhibiting higher strength than expanded clay. This is in line with some studies in the lightweight concrete [1-2], though some studies have found very similar ratios of tensile strength to compressive strength [19]. Finally, the $f_r/\sqrt{f'_c}$ or $f_r/\sqrt{f'_g}$ vs unit weight (of concrete or grout respectively) graph has been presented in figure 6(b) to maintain that the modulus of rupture values for the expanded slate specimens are still consistent with other data found in the literature for lightweight concrete, despite its wider spread and somewhat dissenting behavior from the data that could be obtained from the literature for f_r vs f'_c or f'_g (figure 6(a)).

CONCLUSIONS

This research was focused on determining the performance of anchor bolts under tension in CMU assemblies grouted with lightweight grout. The conclusions drawn are as follows:

1. The TMS 402-16 equations 9-3 to 9-5 correctly predicted the observed masonry tensile break out failure of the bent-bar anchors cast in lightweight grouted specimens and provided conservative estimates for axial tensile strength of the anchor bolt.
2. Masonry tensile break out strength appears to be highly dependent on the lightweight aggregate type used to construct the specimen in addition to the compression strength of the grout.
3. The observed high tensile strength of the expanded slate grout compared to its compression strength is in agreement with other data in the literature for lightweight concrete and there may be potential to account for additional axial tensile anchor bolt capacity when using grouts comprised of these aggregates.

Additional work is planned that will build upon the results of this study by conducting shear testing of bent-bar anchors in grouted assemblies with the same expanded clay and expanded shale grout mixes used in this study. Of interest for future research would be to examine if a definitive relationship between the lightweight aggregate type and tension/shear capacities of bent-bar anchors can be established through additional testing.

ACKNOWLEDGEMENT

We would like to express our deepest appreciation to National Concrete Masonry Association (NCMA) and Expanded Shale, Clay and Slate Institute for funding this project. We are extremely grateful to Jason Thompson from NCMA for his advice throughout the project. We would also like to thank Arcosa Lightweight Aggregate and Stalite Lightweight Aggregate for the generous supply of aggregates for our experiments, and General Shale for block and mortar supplies. Finally, our deepest gratitude to all the helping hands from Dr. Redmond's research group and other colleagues, without whom the experiments would not have been as smooth and as expedient.

REFERENCES

- [1] Clarke, J. L. (1993). *Structural Lightweight Aggregate Concrete* (1st ed.). CRC Press.
- [2] Chandra, S., & Berntsson, L. (2002). *Lightweight Aggregate Concrete* (1st ed.). William Andrew.
- [3] Rashad, A. M. (2018b). Lightweight expanded clay aggregate as a building material – An overview. *Construction and Building Materials*, 170, 757–775.
- [4] Cavalline, T. L., Castrodale, R. W., Freeman, C., & Wall, J. (2017). Impact of Lightweight Aggregate on Concrete Thermal Properties. *ACI Materials Journal*, 114(6), 945–956.
- [5] El Zareef, M. A. (2016). Seismic damage assessment of multi-story lightweight concrete frame buildings reinforced with glass-fiber rods. *Bulletin of Earthquake Engineering*, 15(4), 1451–1470.
- [6] Bentz, D. and Weiss, W. (2011). Internal Curing: A 2010 State-of-the-Art Review. U.S. Department of Commerce. National Institute of Standards and Technology. Gaithersburg, MD.
- [7] De la Varga, I. and Graybeal, B. (2016). Dimensional Stability of Grout-Type Materials Used as Connections between Prefabricated Concrete Elements. Report No. FHWA-HRT-16-008. Federal Highway Administration. Washington, DC.
- [8] Graybeal, B. (2016). Bond of Field-Cast Grouts to Precast Concrete Elements. TechNote No. FHWA-HRT-16-081. Federal Highway Administration. Washington, DC.
- [9] Bentz, D., Jones, S., Peltz, M., & Stutzman, P. (2015) Mitigation of Autogenous Shrinkage in Repair Mortars via Internal Curing. *Concrete in Australia*, 41(4), 35-39.
- [10] Petty, P. B. and Nelson, M. R. (2011). “Structural Lightweight Masonry Grout.” *Proc., 11th North American Masonry Conference*, Minneapolis, USA
- [11] Tanner, A. (2014). *Strength of Masonry Grout Made with Expanded Shale*. MS Thesis, Brigham Young University, USA.
- [12] Polanco, H. J. (2017). *Structural Lightweight Grout Mixture Design*. MS Thesis. Brigham Young University, USA.
- [13] Bane, D. K. (2016). *Material and Structural Properties of Lightweight Masonry Grout*. MS Thesis, Tennessee Technological University, USA.
- [14] Biggs, D. T. (2005). “Grouting Masonry Using Portland Cement-Lime Mortars.” *Proc., International Building Lime Symposium*, Orlando, Florida, USA.
- [15] TMS 402/602-16. (2016), “Building Code Requirements and Specification for Masonry Structures”, The Masonry Society, Longmont, CO, USA.
- [16] McGinley, W.M., Singleton, S., Greenwald, J., Thompson, J. (2004). “Capacity of anchor bolts in concrete masonry.” *Proc., 13th International Brick and Block Masonry Conference*, Amsterdam.
- [17] ACI 613A-59. (1968), “Recommended Practice for Selecting Proportions for Structural Lightweight Concrete”, *ACI Journal*.
- [18] Greene, G. and Graybeal, B. (2013). *Lightweight Concrete: Mechanical Properties*, Report No. FHWA-HRT-13-062, Federal Highway Administration, Washington, DC.
- [19] Byard, B.E. and Schindler A. K. (2010). *Cracking Tendency of Lightweight Concrete*, Highway Research Center, Harbert Engineering Center, Auburn, AL.
- [20] ASTM C476-20. (2020), “Standard Specification for Grout for Masonry”, ASTM International, West Conshohocken, PA.
- [21] ASTM C136/136M-19. (2019), “Standard Test Method for Sieve Analysis of Fine and Coarse Aggregates”, ASTM International, West Conshohocken, PA.

- [22] ASTM C127-15. (2015), “Standard Test Method for Relative Density (Specific Gravity) and Absorption of Coarse Aggregate”, ASTM International, West Conshohocken, PA.
- [23] ASTM C128-15. (2015), “Standard Test Method for Relative Density (Specific Gravity) and Absorption of Fine Aggregate”, ASTM International, West Conshohocken, PA.
- [24] ASTM C1019-19. (2019), “Standard Test Method for Sampling and Testing Grout for Masonry”, ASTM International, West Conshohocken, PA.
- [25] ASTM E488/E488M-18. (2018), “Standard Test Methods for Strength of Anchors in Concrete Elements”, ASTM International, West Conshohocken, PA.
- [26] ASTM E518/E518M-18. (2015), “Standard Test Methods for Flexural Bond Strength of Masonry”, ASTM International, West Conshohocken, PA.